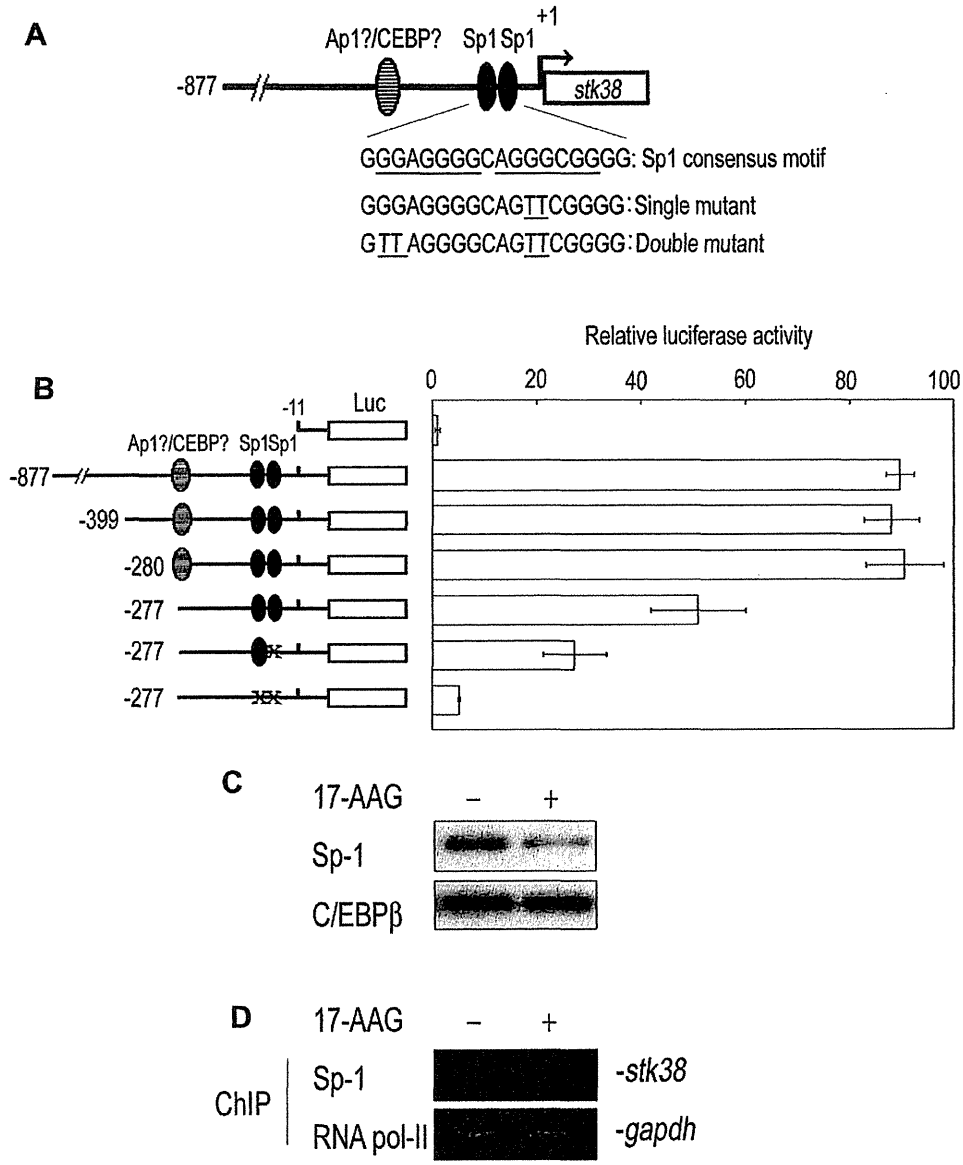

Fig. 3. Functional analysis of the *stk38* promoter. (A) Schematic representation of the human *stk38* promoter, showing putative binding sites for Sp1 transcription factors. (B) Luciferase reporter plasmids containing the human *stk38* promoter with 5′-serial deletions or a mutated Sp1-binding site were transfected into HEK293T cells; after 24 h, luciferase assays were performed on cell lysates. Data obtained from three independent experiments are expressed as the mean ± SD of *Firefly* luciferase values normalised to *Renilla*. (C) Treatment with 17-allylamino-17-demethoxygeldanamycin (17-AAG) decreased Sp1 but not C/EBPβ. HeLa cells were treated with DMSO or 1.0 μM 17-AAG for 12 h, and cell lysates were analyzed by Western blot with the indicated antibodies. (D) Sp1's DNA-binding to the *stk38* promoter is inhibited by 17-AAG. HeLa cells were treated with DMSO or 1.0 μM 17-AAG for 12 h. Sheared chromatin from HeLa cells treated with DMSO or 17-AAG was immunoprecipitated using an antibody against Sp1. The immunoprecipitated DNA was amplified by polymerase chain reaction (PCR) using specific primers targeted to the *stk38* gene promoter elements (nt −277 to −11). RNA polymerase II's DNA-binding to the *gapdh* promoter was used as an internal control.

Sequence analysis showed two Sp1 consensus binding sites in the region between −277 and −11. While site-directed mutagenesis of the Sp1 consensus site G (−63/−62) T moderately reduced the luciferase activity, mutations at both Sp1 consensus sites, G (−73/−72) T and G (−63/−62) T, decreased the luciferase activity to 5.8% of that of the *stk38* promoter containing the region between −877 and −11.

Computational analysis also indicated a putative C/EBPβ-binding site in the −280/−277 region. We next examined the effect of 17-AAG on Sp1 or C/EBPβ expression. As shown in Fig. 3C, treating HeLa cells with 1.0 μM 17-AAG reduced the level of Sp1 but not of C/EBPβ. We then investigated whether the 17-AAG-mediated degradation of Sp1 is proteasome-dependent. We found that MG132 rescued the degrada-

tion of Sp1 (Supplemental Fig. 2). Using a ChIP assay, we found that Sp1 bound to the −277/−11 region of the endogenous *stk38* promoter, and that 1 μM 17-AAG significantly inhibited this binding (Fig. 3D). Thus, Sp1's inability to bind DNA in cells treated with 17-AAG arises from the degradation of Sp1.

3.4. 17-AAG treatment inhibits Sp1-binding activity

Since our results showed that Sp1 binds the endogenous *stk38* promoter, we conducted gel-shift assays to determine whether Sp1 could bind the putative transcription factor sites in the −73/−62 region of the *stk38* promoter. A probe corresponding to the −82/−52 region of the *stk38* promoter formed four complexes, designated I–IV (Fig. 4A, lane 2); these were competed by excess amounts of unlabeled Sp1 consensus oligonucleotides (Fig. 4A, lane 3). A gel-shift assay in the presence of an Sp1-specific antibody showed that complex I was formed by Sp1, as seen from the decrease in signal intensity and the appearance of a super-shifted complex (Fig. 4A, lane 4). Mutating one putative Sp1-binding site—G (−63/−62) T, designated as sm—of the *stk38* promoter had little effect on the formation of complex I, although the mutation diminished the super-shifted complex slightly (Fig. 4A, lanes 5 and 6). Mutations at both putative Sp1-binding sites—G (−73/−72) T and G (−63/−62) T, designated as dm—completely eliminated the formation of complex I and the super-shifted complex (Fig. 4A, lanes 7 and 8). These findings were consistent with the results from the luciferase experiments (Fig. 3B). Complexes II and IV were diminished by adding excess Sp1 consensus oligonucleotides or by using a dm-mutant oligonucleotide as a probe, suggesting that the binding factors of these complexes are Sp1-like proteins. Since introducing mutations had little effect on the formation of complex III, the proteins in complex III may bind at sites other than the Sp1-binding sites. Taken together, our results indicate that Sp1 binds to the −73/−62 region of the *stk38* promoter.

We next used gel-shift assays to investigate the effect of X-ray-irradiation, either alone or in combination with 17-AAG, on Sp1's DNA-binding to the *stk38* promoter. Sp1 from X-irradiated HeLa cells had slightly lower DNA-binding activity than that from unirradiated cells (Fig. 4B, lane 3); in addition, the formation of complex IV increased, suggesting that a rearrangement of binding proteins may occur in this region. Combined treatment with X-ray-irradiation and 17-AAG significantly inhibited the formation of all of the complexes (Fig. 4B, lane 4), indicating that 17-AAG inhibited the binding activity of Sp1 and possibly Sp1-like proteins.

Since the ChIP and gel-shift experiments indicated that 17-AAG inhibited Sp1's DNA-binding activity for the *stk38* promoter, we investigated whether a reduction

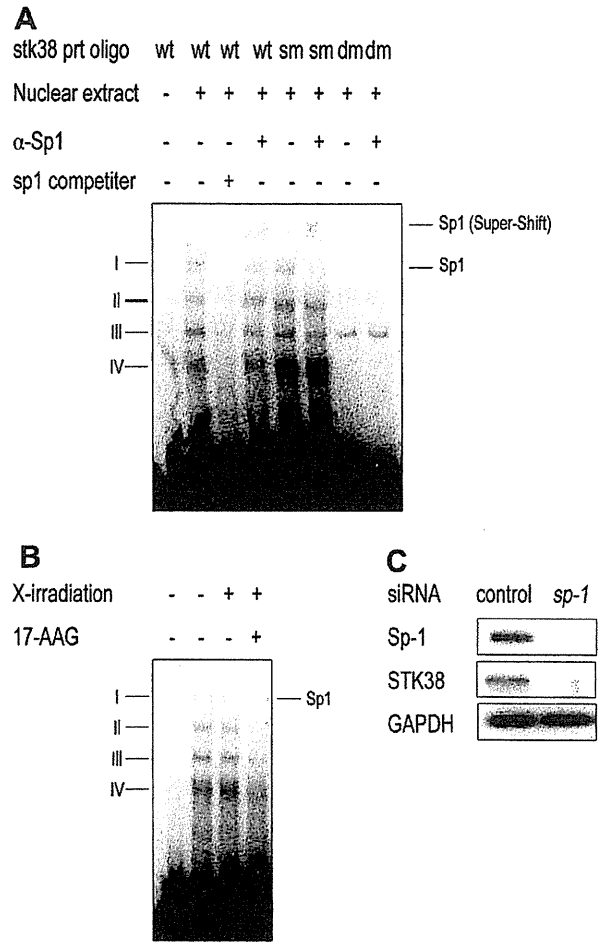

Fig. 4. Sp1's DNA-binding activity is inhibited by 17-allylamino-17-demethoxygeldanamycin (17-AAG). (A) Nuclear extracts were prepared from HeLa cells, and ^{32}P-labeled wild-type oligonucleotides encompassing the Sp1-binding sites at the region (nt −83 to −52) of the *stk38* promoter were incubated in the absence (lane 1) or presence (lane 2) of 5 μg of the nuclear extracts. Competition assays were performed in the presence of a 10× molar excess of cold Sp1 consensus oligonucleotides (lane 3). A super-shift assay was performed by incubating the reaction mixture with 1 μg of Sp1 polyclonal antibody prior to adding the radio-labeled probe (lane 4). Four DNA-protein complexes were formed (I–IV). Mutations were introduced at one or two Sp1-binding sites of the oligonucleotides: G (−63/−62) T (sm), or G (−73/−72) T and G (−63/−62) T (dm). These mutant oligonucleotides were used in gel-shift (lanes 5 and 7) or super-shift assays (lanes 6 and 8). (B) HeLa cells were pretreated with DMSO or 1 μM 17-AAG for 12 h and X-ray-irradiated (20 Gy). Nuclear extracts were prepared 2 h after irradiation. Sp1's DNA-binding activity in untreated, X-ray-irradiated, or 17-AAG-treated irradiated HeLa cells was analyzed by gel-shift assay using ^{32}P-labeled wild-type oligonucleotides. (C) Sp1 knockdown decreases serine/threonine kinase 38 (STK38) expression. HeLa cells were transfected with negative (control) or Sp1 siRNA; 48 h later, cell lysates were prepared and analyzed by Western blot using the indicated antibodies.

in Sp1 activity by *sp1* RNA interference would affect STK38 expression, and found that transfection with *sp1*-specific small interference RNA reduced the STK38 protein level (Fig. 4C). Taken together, our results suggest that 17-AAG suppresses STK38 by

inhibiting Sp1's binding to the promoter of the *stk38* gene.

3.5. 17-AAG inhibits X-ray-stimulated STK38 activity and enhances X-ray-induced cell death by promoting apoptosis

We previously reported that oxidative stress stimulates STK38 activity.[12] To further determine the effect of 17-AAG on X-ray-stimulated STK38 activity, HeLa cells were treated with 1 μM 17-AAG for 12 h and then exposed to a single dose of X-irradiation (20 Gy). Exposing HeLa cells to X-rays alone enhanced STK38's activity slightly (1.4-fold) (Fig. 5A, left panel), but did not affect its protein level. On the other hand, the combination of 17-AAG and X-ray-irradiation significantly decreased STK38's activity, probably because of the 17-AAG-mediated reduction in STK38 levels (Fig. 5A, right panel).

We next conducted colony-formation assays to investigate the impact of 17-AAG and X-ray-irradiation, singly or in combination, on cell survival. HeLa cells were treated with 0.5 μM 17-AAG for 12 h, followed by a single X-ray dose (1, 2, 3, or 5 Gy). Pretreatment with 17-AAG significantly enhanced the X-ray-induced cell death (Fig. 5B, left panel). To further evaluate the radiosensitizing effect of 17-AAG, the RER was measured using the $SF_{0.5}$ determined from the clonogenic assay.

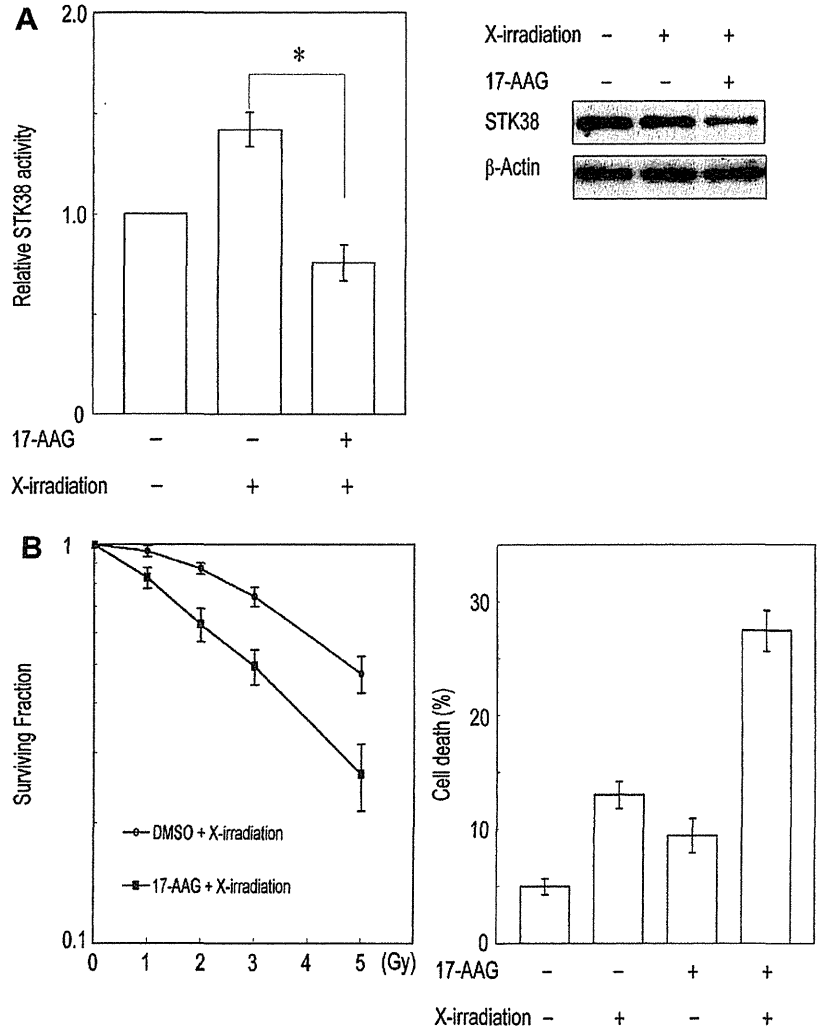

Fig. 5. Treatment with 17-allylamino-17-demethoxygeldanamycin (17-AAG) inhibited X-ray-stimulated serine/threonine kinase 38 (STK38) activity and enhanced radiosensitivity. (A) Left panel: HeLa cells were pretreated with DMSO or 1.0 μM 17-AAG for 12 h, X-ray-irradiated (20 Gy), and incubated an additional 2 h. STK38 kinase activity was measured as described in Fig. 1D. Data represent the average and standard deviations of three independent experiments, expressed as STK38 activity relative to that in cells treated with DMSO only. Statistical analysis was performed using the Student's *t*-test. Asterisks indicate statistically significant differences between X-ray-irradiation only and combined treatment with 17-AAG and X-ray-irradiation ($^*p < 0.05$). Right panel: STK38 levels were analyzed by Western blot. (B) Left panel: Clonogenic assays were performed after HeLa cells were pretreated with DMSO or 0.5 μM 17-AAG for 12 h, X-ray-irradiated at various doses, incubated an additional 2 h. Right panel: HeLa cells were pretreated with DMSO or 0.5 μM 17-AAG for 12 h and X-ray-irradiated (3 Gy); 48 h later, cell death was assessed by staining with Annexin V-FITC plus PI, using a flow cytometer.

The RER for the 17-AAG treatment was 1.64. Previous reports demonstrated that 17-AAG also radiosensitized HCT116 and MCF7 cells.[24,25] We further investigated whether the 17-AAG-mediated radiosensitization was due to enhanced apoptosis. Treatment with either X-ray-irradiation (3 Gy) or 0.5 μM 17-AAG alone induced apoptosis slightly—13.0% and 9.4%, respectively. Importantly, the combination of 17-AAG and X-rays significantly increased the apoptosis (27.5%) (Fig. 5B, right panel).

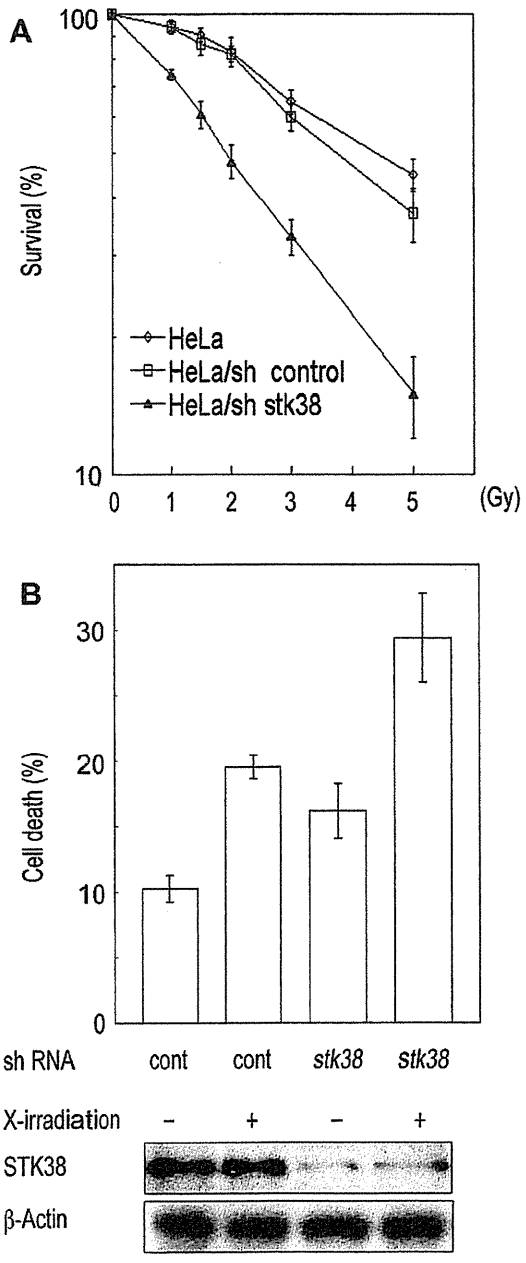

Fig. 6. Serine/threonine kinase 38 (STK38) knockdown enhances X-ray radiosensitivity. (A) HeLa cells were transfected with a non-targeting (control) or *stk38*-specific shRNA expression vector; 24 h later, the cells were placed in culture medium containing 2 μg/ml puromycin and cultured for an additional 48 h. The cells were then either X-ray-irradiated at various doses or left untreated, incubated for an additional 2 h, and assayed for cell survival. (B) HeLa cells were transfected with a non-targeting (control) or *stk38*-specific shRNA expression vector and selected as described above. The shRNA-transfected cells were X-ray-irradiated (3 Gy), and cell death was assessed 48 h later as described in Fig. 5B. STK38 levels were analyzed by Western blot.

3.6. STK38 knockdown enhances X-ray-induced cell death by promoting apoptosis

To clarify the biological significance of *stk38*'s down-regulation, we conducted colony-formation assays to determine the effect of STK38 knockdown on cellular radiosensitivity. Transfection with *stk38* shRNA, but not with a control expression vector, specifically knocked down the endogenous STK38 expression in both unirradiated and X-ray-irradiated HeLa cells. When exposed to X-rays, the cell death increased markedly in the *stk38* shRNA-expressing HeLa cells compared to parental HeLa cells or those expressing control shRNA (Fig. 6A). The RER for the knockdown of STK38 at $SF_{0.5}$ was 2.05. Importantly, the combination of *stk38* shRNA and X-irradiation significantly increased the level of apoptosis (29.5%), as indicated by Annexin V staining, compared to that observed in the parental HeLa cells (11.0%) or those expressing control shRNA (19.0%) (Fig. 6B). Thus, STK38 knockdown radiosensitizes cells by promoting apoptosis.

4. Discussion

In this study, we demonstrated that 17-AAG down-regulated the *stk38* expression by inhibiting Sp1's DNA-binding activity, and that the reduction of STK38 levels enhanced cellular X-ray radiosensitivity. We initially investigated the effect of 17-AAG on STK38, and found that it decreased both the expression and activity of STK38, in a dose- and time-dependent manner. 17-AAG's disruption of HSP90's binding to client proteins is known to destabilize and degrade those client proteins via the ubiquitin–proteasome pathway.[18,19]

Recently, the mammalian NDR/STK38 homologues LATS1 and LATS2 were identified as HSP90 clients, and 17-AAG was shown to reduce their expression.[26] Thus, we investigated whether STK38 was an HSP90 client. The interaction of STK38 and HSP90 was detected in an overexpression but not an endogenous system (data not shown), and treatment with MG132 or lactacystin did not restore the 17-AAG-mediated reduction in STK38 expression. These observations suggested that while STK38 may interact with HSP90, it is not an HSP90 client protein.

We next found that 17-AAG downregulated *stk38*'s expression. The mechanism regulating *stk38*'s

expression has not been clarified. Through 5′-deletion analysis of the *stk38* promoter, we found that the region between −280 and −11 was responsible for the *stk38* promoter activity. This region contained at least two putative Sp1-binding sites. Sp1 is known to bind GC-rich promoter sites, and is considered to be a primary determinant of a promoter's core activity, both by interacting directly with factors in the basal transcriptional machinery and by cooperating with several transcriptional activators.[27,28] In our mutational analysis, the reporter activity decreased slightly with the mutation of one Sp1 site in the *stk38* promoter, G (−63/−62) T. However, mutations at both Sp1-binding sites, G (−73/−72) T and G (−63/−62) T, greatly decreased the promoter activity and Sp1's DNA-binding activity, indicating that both sites are necessary for the transcriptional regulation of the *stk38* promoter.

X-ray-irradiation stimulated the STK38 activity without enhancing its expression, probably through phosphorylation-dependent regulation, as we previously reported.[12] Importantly, 17-AAG decreased STK38 expression through reduction of Sp1's DNA-binding activity to the *stk38* promoter and reduced STK38 activity in both untreated and X-ray-irradiated cells. A previous study showed that HSP90 interacts with Sp1 during mitosis and that the inhibition of HSP90 by geldanamycin induces the ubiquitination and degradation of Sp1.[29] We confirmed that 17-AAG also induced the degradation of Sp1, and that the proteasome inhibitor MG132 rescued the Sp1 levels. These results suggest that HSP90 protects Sp1 from ubiquitin-dependent degradation. Moreover, knocking down Sp1 reduced the STK38 levels, indicating that Sp1 is necessary for STK38's expression.

Based on the involvement of HSP90 in Sp1's stability, our results suggest that 17-AAG downregulates *stk38* expression by decreasing Sp1's binding to the *stk38* promoter; this decreased binding is owing to the proteasome-dependent degradation of Sp1. On the other hand, JNK1, a member of the JNK family,[30] phosphorylates Sp1 to protect it from ubiquitination during mitosis, through an interaction among JNK1, HSP90 and Sp1.[29] Since MG-132 also increases JNK's activity,[31] JNK may be involved in the prevention by MG-132 of Sp1's 17-AAG-induced degradation. JNK is activated by a variety of stimuli, including X-ray-irradiation.[30] However, our results showed that X-irradiation did not stimulate Sp1's binding to the *stk38* promoter. This might have been because X-ray-irradiation induces cell-cycle arrest through the activation of checkpoint machinery and transiently inhibits mitosis,[32] leading to a blockade of the JNK1/HSP90/Sp1 complex formation and of Sp1's phosphorylation by JNK during mitosis.

Since the *stk38* promoter activity decreased 43% with the 5′-deletion of the region between −280 and −277, suggesting that another *cis*-acting element exists in this region, we searched for putative transcription factor-binding sites that might support this activity. Computer analysis revealed several potential elements, including Ap1- and C/EBP-binding sites. Ap1 activity is stimulated by oxidative stresses or PMA treatment.[28] However, neither X-ray-irradiation nor PMA treatment stimulated the *stk38* promoter activity, indirectly suggesting that Ap1 is not involved in regulating the *stk38* promoter. We also found that 17-AAG treatment did not alter the expression of the C/EBP isoform C/EBPβ. This result suggested that C/EBPβ is not responsible for the *stk38* downregulation mediated by 17-AAG, although it might be required for the *stk38* promoter's basal activity.

Preclinical studies have shown that 17-AAG can enhance tumor-cell sensitivity to radiation, while reducing the expressions of radioresistance-associated proteins such as Akt, Raf-1, and Hif-1α.[33,34] Our present study showed that 17-AAG radiosensitized HeLa cells and reduced STK38 expression and that knocking down STK38 significantly enhanced the X-ray radiosensitivity by promoting apoptosis. These results suggest that STK38 is a radioresistance-associated protein. We previously demonstrated that STK38 interacts with and negatively regulates several JNK kinase kinases and that STK38 knockdown enhances stress-induced JNK signaling.[12,13] JNKs are directly linked to cell death.[35] Thus, the 17-AAG-mediated decrease in STK38 or knockdown of *stk38* could activate JNK signaling, leading to an enhancement of X-ray-induced apoptosis. Knocking down *stk38* had a strong radiosensitizing effect, greater than that mediated by 17-AAG, possibly due to differences in the residual STK38 expression levels. The STK38 expression was partially eliminated by 17-AAG treatment, but it was completely eliminated by transfection with an *stk38* shRNA expression vector. Consistent with our results, a recent study demonstrated that silencing STK38 suppresses tumor growth accompanied by increased apoptosis in an *in vivo* mouse xenograft model.[36]

Since Sp1 is a general transcription factor, it is not particularly suitable for molecular targeting in radiotherapy. On the other hand, STK38 regulates centrosome duplication and protects cells from oxidative stress.[12,37] Moreover, STK38 is upregulated in progressive ductal carcinoma *in situ* and in some melanoma cell lines.[38,39] Thus, radiotherapy and STK38-targeted therapies may have synergistic effects. STK38's substrates and downstream factors still need to be clarified. Our results indicate that STK38 is required to prevent cell death in response to X-irradiation and suggest a new pathway for 17-AAG-mediated radiosensitization via *stk38* downregulation.

Conflict of interest statement

None declared.

Acknowledgements

We thank Dr. Yoshihiro Fujii (Ibaraki Prefectural University of Health Sciences) for helpful discussions and for providing reagents. This work was supported in part by a Grant-in-Aid for Scientific Research (20591491) from the Ministry of Education, Culture, Sports, Science, and Technology of Japan to A.E.

Appendix A. Supplementary data

Supplementary data associated with this article can be found, in the online version, at http://dx.doi.org/10.1016/j.ejca.2013.06.034.

References

1. Manning G, Plowman GD, Hunter T, Sudarsanam S. Evolution of protein kinase signaling from yeast to man. *Trends Biochem Sci* 2002;**27**:514–20.
2. Tamaskovic R, Bichsel SJ, Hemmings BA. NDR family of AGC kinases—essential regulators of the cell cycle and morphogenesis. *FEBS Lett* 2003;**546**:73–80.
3. Hergovich A, Stegert MR, Schmitz D, Hemmings BA. NDR kinases regulate essential cell processes from yeast to humans. *Nat Rev Mol Cell Biol* 2006;**7**:253–64.
4. Verde F, Wiley DJ, Nurse P. Fission yeast *orb6*, a ser/thr protein kinase related to mammalian rho kinase and myotonic dystrophy kinase, is required for maintenance of cell polarity and coordinates cell morphogenesis with the cell cycle. *Proc Natl Acad Sci USA* 1998;**95**:7526–31.
5. Bidlingmaier S, Weiss EL, Seidel C, Drubin DG, Snyder M. The Cbk1p pathway is important for polarized cell growth and cell separation in *Saccharomyces cerevisiae*. *Mol Cell Biol* 2001;**21**:2449–62.
6. Johnston LH, Eberly SL, Chapman JW, Araki H, Sugino A. The product of the *Saccharomyces cerevisiae* cell cycle gene *DBF2* has homology with protein kinases and is periodically expressed in the cell cycle. *Mol Cell Biol* 1990;**10**:1358–66.
7. Stegert MR, Tamaskovic R, Bichsel SJ, Hergovich A, Hemmings BA. Regulation of NDR2 protein kinase by multi-site phosphorylation and the S100B calcium-binding protein. *J Biol Chem* 2005;**279**:23806–12.
8. Ultanir SK, Hertz NT, Li G, et al. Chemical genetic identification of NDR1/2 kinase substrates AAK1 and Rabin8 uncovers their roles in dendrite arborization and spine development. *Neuron* 2012;**73**:1127–42.
9. Stegert MR, Hergovich A, Tamaskovic R, Bichsel SJ, Hemmings BA. Regulation of NDR protein kinase by hydrophobic motif phosphorylation mediated by the mammalian Ste20-like kinase MST3. *Mol Cell Biol* 2005;**25**:11019–29.
10. Bichsel SJ, Tamaskovic R, Stegert MR, Hemmings BA. Mechanism of activation of NDR (nuclear Dbf2-related) protein kinase by the hMOB1 protein. *J Biol Chem* 2004;**279**:35228–35.
11. Devroe E, Erdjument-Bromage H, Tempst P, Silver PA. Human Mob proteins regulate the NDR1 and NDR2 serine–threonine kinases. *J Biol Chem* 2004;**279**:24444–51.
12. Enomoto A, Kido N, Ito M, Takamatsu N, Miyagawa K. Serine–threonine kinase 38 is regulated by glycogen synthase kinase-3 and modulates oxidative stress-induced cell death. *Free Radic Biol Med* 2012;**52**:507–15.
13. Enomoto A, Kido N, Ito M, et al. Negative regulation of MEKK1/2 signaling by serine–threonine kinase 38 (STK38). *Oncogene* 2008;**27**:1930–8.
14. Calderwood SK, Khaleque MA, Sawyer DB, Ciocca DR. Heat shock proteins in cancer: chaperones of tumorigenesis. *Trends Biochem Sci* 2006;**31**:164–72.
15. Pearl LH, Prodromou C, Workman P. The Hsp90 molecular chaperone: an open and shut case for treatment. *Biochem J* 2008;**410**:439–53.
16. Wandinger SK, Richter K, Buchner J. The Hsp90 chaperone machinery. *J Biol Chem* 2008;**283**:18473–7.
17. Kim YS, Alarcon SV, Lee S, et al. Update on Hsp90 inhibitors in clinical trial. *Curr Top Med Chem* 2009;**9**:1479–92.
18. Whitesell L, Lindquist SL. HSP90 and the chaperoning of cancer. *Nat Rev Cancer* 2005;**5**:761–72.
19. Sharp S, Workman P. Inhibitors of the HSP90 molecular chaperone: current status. *Adv Cancer Res* 2006;**95**:323–48.
20. Neckers L. Hsp90 inhibitors as novel cancer chemotherapeutic agents. *Trends Mol Med* 2002;**8**:S55–61.
21. Kamal A, Thao L, Sensintaffar J, et al. A high-affinity conformation of Hsp90 confers tumor selectivity on Hsp90 inhibitors. *Nature* 2003;**425**:407–10.
22. Kabakov AE, Makarova YM, Malyutina YV. Radiosensitization of human vascular endothelial cells through Hsp90 inhibition with 17-*N*-allilamino-17-demethoxygeldanamycin. *Int J Radiat Oncol Biol Phys* 2008;**71**:858–65.
23. Noguchi M, Yu D, Hirayama R, et al. Inhibition of homologous recombination repair in irradiated tumor cells pretreated with Hsp90 inhibitor 17-allylamino-17demethoxygeldanamycin. *Biochem Biophys Res Commun* 2006;**351**:658–63.
24. Stecklein SR, Kumaraswamy E, Behbod F, et al. Brca1 and Hsp90 cooperate in homologous and non-homologous DNA double-strand-break repair and G2/M checkpoint activation. *Proc Natl Acad Sci USA* 2012;**109**:13650–5.
25. Moran DM, Gawlak G, Jayaprakash MS, Mayar S, Maki CG. Geldanamycin promotes premature mitotic entry and micronucleation in irradiated p53/p21 deficient colon carcinoma cells. *Oncogene* 2008;**27**:5567–77.
26. Huntoon CJ, Nye MD, Geng L, et al. Heat shock protein 90 inhibition depletes LATS1 and LATS2, two regulators of the mammalian hippo tumor suppressor pathway. *Cancer Res* 2010;**70**:8642–50.
27. Suske G. The Sp-family of transcription factors. *Gene* 1999;**238**:291–300.
28. Dunah AW, Jeong H, Griffin A, et al. Sp1 and TAFII130 transcriptional activity disrupted in early Huntington's disease. *Science* 2002;**296**:2238–43.
29. Wang SA, Chuang JY, Yeh SH, et al. Heat shock protein 90 is important for Sp1 stability during mitosis. *J Mol Biol* 2009;**387**:1106–19.
30. Davis RJ. Signal transduction by the JNK group of MAPK kinases. *Cell* 2000;**103**:239–52.
31. Meriin AB, Gabai VL, Yaglom J, Shifrin VI, Sherman MY. Proteasome inhibitors activate stress kinases and induce Hsp72. *J Biol Chem* 1998;**273**:6373–9.
32. Bartek J, Lukas J. DNA damage checkpoints: from initiation to recovery or adaptation. *Curr Opin Cell Biol* 2007;**19**:238–45.
33. Russel JS, Burgan W, Oswald KA, Camphausen K, Tofilon PJ. Enhanced cell killing induced by the combination of radiation and the heat shock protein 90 inhibitor 17-allylamino-17-demethoxygeldanamycin: a multitarget approach to radiosensitization. *Clin Cancer Res* 2003;**9**:3794–800.
34. Kim WY, Oh SH, Woo JK, Hong WK, Lee HY. Targeting heat shock protein 90 overrides the resistance of lung cancer cells by blocking radiation-induced stabilization of hypoxia-inducible factor-1α. *Cancer Res* 2009;**69**:1624–32.
35. Tournier C, Hess P, Yang DD, et al. Requirement of JNK for stress-induced activation of the cytochrome c-mediated death pathway. *Science* 2000;**288**:870–4.
36. Bisikirska BC, Adam SJ, Alvarez MJ, et al. STK38 is a critical upstream regulator of Myc's oncogenic activity in human B-cell

lymphoma. *Oncogene* 2012, advance online publication, 26 November, 2012.
37. Hergovich A, Lamla S, Nigg EA, Hemmings BA. Centrosome-associated NDR kinase regulates centrosome duplication. *Mol Cell* 2007;**25**:625–34.
38. Millward TA, Heizmann CW, Schafer BW, Hemmings BA. Calcium regulation of Ndr protein kinase mediated by S100 calcium-binding proteins. *EMBO J* 1998;**17**:5913–22.
39. Adeyinka A, Emberley E, Niu Y, et al. Analysis of gene expression in ductal carcinoma in situ of the breast. *Clin Cancer Res* 2002;**8**:3788–95.

Comparison of the bromodeoxyuridine-mediated sensitization effects between low-LET and high-LET ionizing radiation on DNA double-strand breaks

YOSHIHIRO FUJII[1,2], MATTHEW D. GENET[3], ERICA J. ROYBAL[3], NOBUO KUBOTA[1], RYUICHI OKAYASU[4], KIYOSHI MIYAGAWA[2], AKIRA FUJIMORI[4] and TAKAMITSU A. KATO[3]

[1]Department of Radiological Sciences, Ibaraki Prefectural University of Health Sciences, Inashiki, Ibaraki 300-0394; [2]The University of Tokyo, Graduate School of Medicine, Bunkyo, Tokyo 113-0033, Japan; [3]Department of Environmental and Radiological Health Sciences, Colorado State University, Fort Collins, CO 80523, USA; [4]National Institute of Radiological Sciences, Research Center for Charged Particle Therapy, International Open Laboratory, Anagawa Inage, Chiba 263-8555, Japan

Received November 13, 2012; Accepted December 17, 2012

DOI: 10.3892/or.2013.2354

Abstract. The incorporation of halogenated pyrmidines such as bromo- and iodo-deoxyuridines (BrdU, IdU) into DNA as thymidine analogs enhances cellular radiosensitivity when high-linear energy transfer (LET) radiation is not used. Although it is known that high-LET ionizing radiation confers fewer biological effects resulting from halogenated pyrimidine incorporation, the exact mechanisms of reduced radiosensitivity with high-LET radiation are not clear. We investigated the radiosensitization effects of halogenated pyrimidines with high-LET radiation using accelerated carbon and iron ions. Cells synchronized into the G_1 phase after unifilar (1 cell cycle) and bifilar (2 cell cycles) substitution with 10 μM BrdU were exposed to various degrees of LET with heavy ions and X-rays. We then carried out a colony formation assay to measure cell survival. The γ-H2AX focus formation assay provided a measure of DNA double-strand break (DSB) formation and repair kinetics. Chromosomal aberration formations for the first post-irradiation metaphase were also scored. For both low-LET X-rays and carbon ions (13 keV/μm), BrdU incorporation led to impaired DNA repair kinetics, a larger initial number of DNA DSBs more frequent chromosomal aberrations at the first post-irradiated metaphase, and increased radiosensitivity for cell lethality. The enhancement ratio was higher after bifilar substitution. In contrast, no such synergistic enhancements were observed after high-LET irradiation with carbon and iron ions (70 and 200 keV/μm, respectively), even after bifilar substitution. Our results suggest that BrdU substitution did not modify the number and quality of DNA DSBs produced by high-LET radiation. The incorporation of halogenated pyrimidines may produce more complex/clustered DNA damage along with radicals formed by low-LET ionizing radiation. In contrast, the severity of damage produced by high-LET radiation may undermine the effects of BrdU and account for the observed minimal radiosensitization effects.

Correspondence to: Dr Takamitsu A. Kato, Department of Environmental and Radiological Health Sciences, Colorado State University, 1618 Campus Delivery, Fort Collins, CO 80523, USA
E-mail: tkato@rams.colostate.edu

Key words: bromodeoxyuridine, linear energy transfer, double-strand break

Introduction

Halogenated pyrimidines are well known as classic radiosensitizers for low-linear energy transfer (LET) radiation such as X-rays and γ-rays (1-4). They also have strong sensitization effects for visible and ultraviolet light (5-7). The mechanisms of bromodeoxyuridine (BrdU)-mediated radiosensitization have been explained elsewhere (8-12). Simply put, single-strand break formation from BrdU-mediated radicals results in the formation of lethal DNA double-strand breaks (DSBs). Since sensitization can be partially reduced by adding radical scavengers such as acetone, various reports suggest that BrdU either produces lethal DSBs or fixes potentially lethal damage (PLD) to enhance cell killing (13-16).

High-LET radiation has a strong effect on cell killing when compared to low-LET radiation. Namely, it achieves a higher relative biological effectiveness (RBE) than low-LET radiation (17-20) by producing dense ionization and causing complex, clustered DNA damage (21-24). However, the complex clustered damage produced by high-LET radiation is not fully understood (21). Radiosensitizers are typically less effective when using high-LET radiation when compared with low-LET radiation (25,26).

Reports have indicated that the incorporation of halogenated pyrimidines not only increases the magnitude of radiation-induced DNA damage, but also suppresses DNA damage repair (2,9,16). High-LET radiation produces 'clustered damage', a type of DNA damage which is also difficult to repair (2,9,16). LET-dependent sensitization of halogenated pyrimidines is reported in cellular lethality (25). As LET

increases, increased clustered DNA damage is formed. At LET >100 keV/μm, the RBE declines as LET increases (27,28).

We hypothesized that the mechanism of BrdU-induced hypersensitivity to ionizing radiation is based on the quality of DNA DSBs. We examined the effects of combinations of high-LET heavy ions and unifilar and bifilar BrdU substitution in Chinese hamster ovary (CHO) cells to better understand the BrdU dependency. In this study, we revealed that BrdU substitution followed by low-LET radiation altered DNA damages into more complex damages similar to those observed after high-LET radiation exposure only, while no additional effects on cellular lethality, chromosomal aberrations and DNA DSB formation and repair were observed following high-LET radiation with BrdU.

Materials and methods

Cell lines and culture. Chinese Hamster ovary (CHO10B2) cells (wild-type) were kindly supplied by Dr Joel Bedford of Colorado State University (Fort Collins, CO, USA). Cells were grown in αMEM (Invitrogen, Carlsbad, CA, USA) supplemented with 10% heat-inactivated (56˚C for 30 min) fetal bovine serum (FBS, Sigma, St. Louis, MO, USA) and 1% antibiotics and antimycotics (Invitrogen) in a humidified 5% CO_2 atmosphere at 37˚C. Cell doubling time was ~12 h.

Irradiation and drug treatment. Cells were cultured in a moderately toxic concentration of BrdU (10 μM, Sigma, St. Louis, MO, USA) for our experiments. Log phase cells were cultured in 10 μM BrdU for 10 or 20 h before synchronization to achieve unifilar (>95%) or bifilar (~95%) substitution, respectively. The substitution of BrdU was confirmed by immunocytochemistry against the BrdU antibody (BD, Franklin Lakes, NJ, USA) for unifilar and fluorescence plus Giemsa (FPG) differential staining on metaphase chromosomes for bifilar (29). Cell cycle synchronization was achieved by the mitotic shake-off method (30). Two hours after shake-off, >95% of cells were synchronized in the G_1 phase before they were exposed to ionizing radiation. Cell synchronization was confirmed by flow cytometry. The Titan X-ray irradiator (200 kVp, 20 mA, 0.5-mm Al and 0.5-mm Cu filters; Shimadzu, Japan) yields an X-ray dose of ~1 Gy/min at room temperature. For heavy ion exposure, accelerated ions were irradiated using the Heavy Ion Medical Accelerator in Chiba (HIMAC) at room temperature. Radiation exposure was carried out in a dark environment to prevent cellular toxicity from room light. Dosimetry and beam quality tests for heavy ions were carried out and confirmed by operators of Accelerator Engineering Corp. (Chiba, Japan) (31-34).

Chromosomal aberration assay. To achieve first metaphase arrest, post-irradiated cells were treated with 0.1 μg/ml Colcemid (Sigma) 10-16 h after irradiation. The cells were treated with 75 mM KCl for 15 min at 37˚C. After hypotonic treatment, the cells were fixed with fixative [methanol:acetic acid solution (3:1)] three times and were dropped onto slides. The samples were stained with filtered 10% (v/v) Giemsa solution in Gurr solution (Invitrogen). At least 30 metaphase cells were scored in at least three separate experiments. Chromosomal aberrations were scored as dicentric, fragment, ring, and interstitial and terminal deletion and pooled as total chromosomal aberrations per cell.

Colony formation assay. Cells were trypsinized and plated into P-60 cell culture dishes immediately after the ionizing radiation exposure. Approximately one week later, cells were fixed with 100% ethanol and stained with crystal violet for colony counting. Colonies containing >50 cells were counted as survivors. Plating efficiency was ~75% for the control and 70% for both unifilar and bifilar cells. RBE was calculated from doses required to achieve 10% survival fraction, and the sensitization enhancement ratio (SER) was calculated from the doses required to achieve 37% cell survival.

γ-H2AX formation assay. Synchronized cells were grown on chamber slides for 2 h. After irradiation of 1 Gy and various incubation times (1, 2, or 3 h post-irradiation), the cells were fixed and stained as previously described (35,36). Cellular imaging was accomplished using an Olympus FV300 fluorescence confocal microscope equipped with an Olympus Fluoview three dimensional image analysis system (Olympus, Tokyo, Japan). The foci were scored in at least 50 cells per data point. Three to four independent experiments were carried out.

Statistical analysis. Statistical comparison of mean values was performed using a t-test. Differences with a P-value of <0.05 were considered to indicate a statistically significant result. Error bars indicate standard error of the means. Confidence interval values were calculated by Prism 5™ software (GraphPad, La Jolla, CA, USA).

Results

Comparison of the BrdU substitution-induced radiosensitization effect with X-rays and heavy ions in a colony formation assay. For X-rays and carbon ions with LET of 13 keV/μm, BrdU-incorporated cells were more sensitive to ionizing radiation when compared with the BrdU-negative controls (Fig. 1A and B). Both the initial shoulder and slope of the survival curves were affected by BrdU incorporation. The sensitization effect of BrdU bifilar substituted cells was stronger than unifilar incorporation. In contrast, for higher LET using heavy ions such as carbon ions at LET of 70 keV/μm or iron ions at LET of 200 keV/μm, BrdU substitution did not induce synergistic sensitization with ionizing radiation (Fig. 1C and D). The D_{10} value, the dose which resulted in 10% cell survival and the D_{37}, value, the dose which resulted in 37% cell survival, decreased depending on the level of BrdU incorporation (Table I). For example, the D_{10} value of 5.4 for X-irradiated unlabeled cells was reduced to 3.6 in bifilarly labeled cells, and that of 4.9 for 13 keV/μm LET carbon ion-exposed unlabeled cells was reduced to 3.4 in bifilarly labeled cells. For high-LET radiation, the change in D_{10} value of LET 70 keV/μm carbon ions was from 2.7 to 2.3, and that of LET 200 keV/μm iron ions was from 2.4 to 2.1 for unlabeled to bifilar BrdU substitution. Differences between sets of D_{10} values were statistically significant. On the other hand, for the D_{37} values of unlabeled and bifilar BrdU substitution for high-LET carbon and iron ions, differences between them were regarded as statistically not significant.

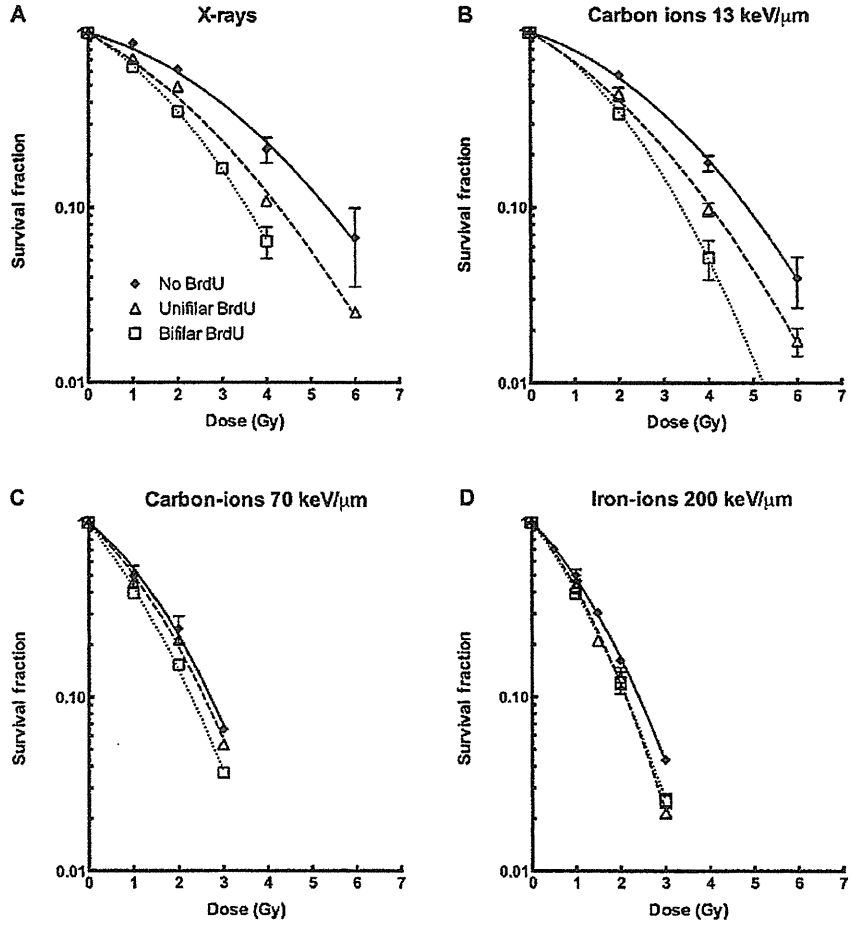

Figure 1. Clonogenic survival curves for different radiation qualities and BrdU incorporation. (A) X-rays, (B) LET 13 keV/μm carbon ions, (C) LET 70 keV/μm carbon ions, (D) LET 200 keV/μm iron ions. ◆, No BrdU substitution; Δ, unifilar substitution; □, bifilar substitution. Three to five independent experiments were carried out. Error bars indicate standard error of the means. Error bars smaller than symbols are not visible. Curves were drawn by GraphPad Prism 5 with linear quadratic regression.

Table I. Relationship between the D_{10} and D_{37} values and BrdU incorporation for different radiation qualities.

Radiation	D_{10}, D_{37}	No BrdU	Unifilar BrdU	Bifilar BrdU
X-ray	D_{10}	5.4 (4.89-5.86)	4.3 (4.08-4.45)	3.6 (3.39-3.72)
	D_{37}	3.1 (2.49-3.58)	2.3 (2.00-2.51)	1.9 (1.68-2.15)
Carbon ions	D_{10}	4.9 (4.46-5.20)	4.1 (3.77-4.28)	3.4 (2.98-3.66)
13 keV/μm	D_{37}	2.9 (2.16-3.33)	2.2 (1.80-2.50)	1.9 (1.48-2.30)
Carbon ions	D_{10}	2.7 (2.47-2.96)	2.6 (2.46-2.68)	2.3 (2.20-2.36)
70 keV/μm	D_{37}	1.5 (1.13-1.74)	1.4 (1.21-1.49)	1.1 (1.02-1.25)
Iron ions	D_{10}	2.4 (2.33-2.49)	2.1 (1.99-2.23)	2.1 (1.97-2.24)
200 keV/μm	D_{37}	1.3 (1.18-1.38)	1.1 (0.95-1.29)	1.2 (0.89-1.25)

D_{10} and D_{37} values were calculated from GraphPad Prism 5. Mean and 99% confidence interval are shown. Experiments were carried out at least three times to obtain the data.

Comparison of BrdU substitution-induced radiosensitization effect with X-rays and heavy ions in a chromosomal aberration assay. As previously shown in the colony formation assay, BrdU-mediated radiosensitization was impaired as LET increased (Fig. 1C and D). To further investigate the mechanism of cell killing, we analyzed first post-irradiation metaphase chromosomes with a chromosomal aberration assay. As predicted from the survival data, no additional

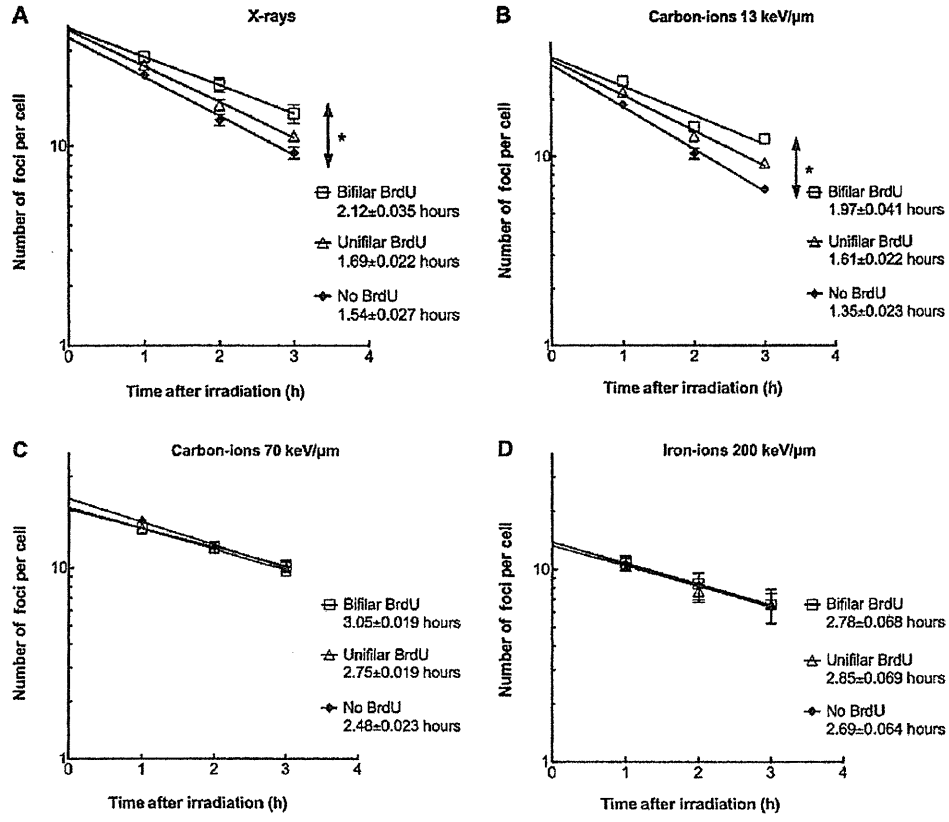

Figure 2. γ-H2AX focus formation assay. (A) X-rays, (B) LET 13 keV/μm carbon ions, (C) LET 70 keV/μm carbon ions, (D) LET 200 keV/μm iron ions. ◆, No BrdU substitution; Δ, unifilar substitution; □, bifilar substitution. Half-life and standard error of the means are shown. Three to four independent experiments were carried out. Error bars indicate standard error of the means. Error bars smaller than symbols are not visible. *Statistical significance ($P<0.05$, t-test) between 0 and 1 cycle and between 0 and 2 cycles of BrdU incorporation.

Table II. Chromosomal aberration assay in first post-irradiation metaphase following irradiation at G1 phase with BrdU substitutions.

Radiation	Dose	No BrdU	Unifilar	Bifilar
No irradiation	0 Gy	0.05±0.03	0.11±0.05	0.15±0.05
X-ray	1 Gy	0.30±0.03	0.48±0.03	0.71±0.04
	2 Gy	0.75±0.05	1.01±0.06	1.33±0.04
Carbon ions	1 Gy	0.42±0.05	0.80±0.20	1.00±0.00
13 keV/μm	2 Gy	1.06±0.17	1.56±0.24	1.93±0.12
Carbon ions	1 Gy	1.26±0.13	1.30±0.25	1.23±0.09
70 keV/μm	2 Gy	2.12±0.31	2.54±0.69	2.73±0.37
Iron ions	1 Gy	1.34±0.21	1.26±0.26	1.40±0.47
200 keV/μm	2 Gy	2.84±0.13	2.68±0.79	2.70±0.64

More than 30 metaphase cells were scored in at least three independent experiments and calculated standard errors of mean.

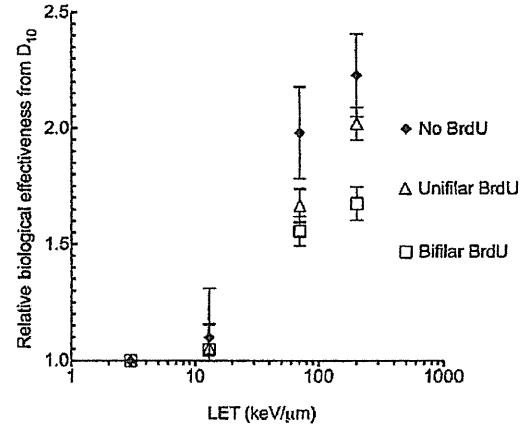

Figure 3. RBE values for different qualities of radiation. RBE values were calculated from the dose to achieve 10% survival. Error bars indicate standard errors of the means.

chromosomal aberrations were observed after BrdU substitution and subsequent high-LET radiation exposure (Table II). After X-ray or LET 13 keV/μm carbon ion exposure, BrdU substitution-mediated radiosensitization was observed at each dose point (1 and 2 Gy) with BrdU incorporation. For instance, bifilar incorporation at 2 Gy increased chromosomal aberrations by 1.71- (from 0.75 to 1.33) and 1.82-fold (from 1.06 to 1.93) for X-rays and LET 13 keV/μm carbon ions, respectively. In contrast, there was almost no radiosensitization at any dose or incorporation time as a result of carbon (70 keV/μm) or iron (200 keV/μm) ions.

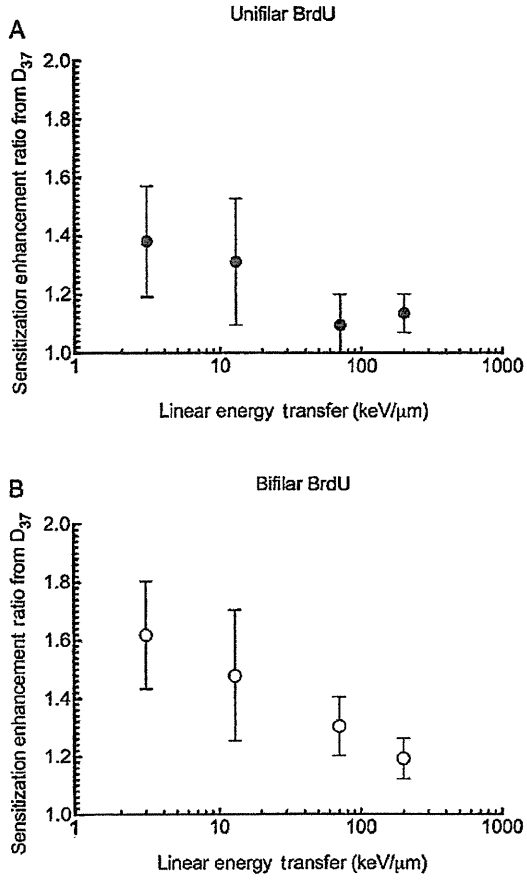

Figure 4. SER values for different qualities of radiation with unifilar (A) or bifilar (B) BrdU substitution. SER values were calculated from the dose to achieve 37% survival, which means the average of one lethal dose per population. Error bars indicate standard errors of the means.

Comparison of BrdU-induced enhancement effect with X-rays and heavy ions in the γ-H2AX formation assay. DNA DSBs result in chromosomal aberrations and cell killing. To investigate the initial amount of DNA damage and DNA repair efficiency following various radiation exposures, we performed a γ-H2AX foci formation assay. One hour after X-ray exposure 22.6 foci per cell for controls, 25.5 foci per cell for unifilar substitution (13% increase), and 27.8 foci per cell for bifilar incorporation (23% increase) were scored. At 3 h after irradiation, the numbers of foci remaining were 9.2 for controls, 12.1 for unifilar incorporation (32% increase), and 14.5 foci for bifilar incorporation (58% increase) (Fig. 2). For LET 13 keV/μm carbon ions, the number of γ-H2AX foci was 18.2 and 6.6 for controls, 21.5 (18% increase) and 9.3 (41% increase) for single BrdU incorporation, and 24.1 (52% increase) and 12.1 (83% increase) for double incorporation at 1 and 3 h, respectively (Fig. 2). Low-LET radiation resulted in an increased number of initial BrdU-induced DNA DSBs and an increased amount of damage remaining in BrdU-incorporated cells. In contrast, high-LET radiation resulted in no significant difference in the number of initial BrdU-induced DNA DSBs or damage remaining in the BrdU-incorporated cells (Fig. 2).

To estimate the effects on repair capacity resulting from BrdU substitution, we calculated half-lives for the reduction of γ-H2AX foci between 1 and 3 h post-irradiation (Fig. 2). Half lives for low-LET exposures increased with the amount of BrdU substitution (from 1.54 to 2.12 h for X-ray bifilar and 1.35 to 1.97 h for bifilar LET 13 keV/μm carbon-ions). In contrast, high-LET exposures (iron-ions in particular) showed no significant difference in γ-H2AX foci half-lives with or without BrdU substitution (from 2.69 to 2.78 h, $P<0.05$).

BrdU substitution effects RBE and SER. In order to assess BrdU substitution effects on radiosensitization, RBE and SER values were obtained. Without BrdU substitution, CHO10B2 cells showed a maximum of an ~2.1 RBE value at LET 200 keV/μm. The LET values were decreased when cells were incorporated with unifilar or bifilar BrdU. The degree of reduction was stronger for bifilar BrdU substitution than unifilar BrdU substitution (Fig. 3). SER values showed that unifilar BrdU substitutions are ~1.4 more effective in cell killing when compared to values without substitution with X-ray exposure, while there was only a 1.1 increase in effectiveness with high LET radiation such as carbon 70 keV/μm and iron ions 200 keV/μm (Fig. 4). The same trend was observed for bifilar substitution. The SER values were decreased from 1.6 to 1.2.

Discussion

In order to investigate the reduced synergistic effects of a combination of high-LET radiation and BrdU incorporation, we compared the damage resulting from low- or high-LET radiation exposure with and without BrdU substitution with several endpoints. We showed that BrdU substitution mediated radiosensitization effects on low-LET photon radiation and particle radiation but similar cellular lethality was observed after high-LET radiation (Fig. 1). Linstadt *et al* (25) proved that the extent of radiosensitization caused by IdU, a halogenated pyrimidine, decreased as the LET increased. In addition, they found very small sensitization enhancements for the distal peak (82 keV/μm) and Bragg peak (183 keV/μm) of a Neon ion beam and no radiosensitization was observed for an extremely high-LET Lanthanum ion beam with 1000 keV/μm (25). Our study was consistent with these results as carbon ions with LET 70 keV/μm and iron ions with LET 200 keV/μm following unifilar or bifilar BrdU incorporation yielded very weak radiosensitization for cellular lethality. Fig. 3 shows the RBE values calculated from D_{10} with BrdU substitution (Table I). Smaller RBE values were noted after high-LET radiation exposure with BrdU substitution. Among the same BrdU substituted cells, high-LET and high RBE advantage was lost. The SER values for high-LET were smaller when cells were incorporated with more BrdU (Fig. 4A and B). When halogenated pyrimidine is used for clinical practice, it is worthy to note that enhancement of cell killing would be smaller using carbon ion radiotherapy than that expected in X-ray radiotherapy. Normal tissues incorporated with BrdU would be severely sensitized following low-LET exposure. Therefore, the dose to patients should be reduced to avoid adverse side effects.

Fig. 2 shows that initial (1 h post-irradiation) DNA damage observed as phosphorylated H2AX foci was increased with BrdU incorporation degrees only for low-LET radiation but not high-LET radiation. Therefore, we assume that initial DNA damages are increased with BrdU substitution for low-LET radiation but not for high-LET radiation. This result was

consistent with other reports (4,15). As a result of more initial damage and slower repair, there were additional γ-H2AX foci in BrdU substituted cells after low-LET radiation. γ-H2AX foci are excellent markers for DNA double-strand breaks. H2AX is phosphorylated ~2 mega bases from a DSB site (35,36). We could not exclude the possibility that additional DSBs were produced by BrdU sensitization following high-LET radiation within short range to be recognized as a single focus.

In order to evaluate DNA repair kinetics, we calculated the half-life of γ-H2AX foci from 1 to 3 h after irradiation (Fig. 2). Many DNA DSB repair deficient mutants were found to have slower kinetics of DSB repair and γ-H2AX foci disappearance (37-39). Half-lives of γ-H2AX foci were affected by BrdU substitutions for low-LET radiation, but not for high-LET radiation (Fig. 2). The results coincide with other studies, suggesting that slower repair is one of the possible mechanisms for BrdU-induced radiosensitization (2,13,16,40). In contrast, one study found that halogenated pyrimidines did not effect the repair of PLD for low-LET radiation (X-rays and neon ions with LET 38 keV/μm) and sublethal damage repair (25).

We clearly observed that the combination of BrdU and high-LET radiation does not increase the half-life of γ-H2AX foci disappearance any more than high-LET radiation alone. This suggests that the BrdU substitution did not modify DNA DSBs produced by high-LET radiation or such modifications were naturally formed by high-LET radiation. Multiple publications suggest that high-LET radiation produces dense ionization in their tracks and produce multiple damages near DNA double-strand breaks and form clustered and complex damage (4,12,22,41). These damages are very difficult to repair and it results in high lethality per absorbed physical dose. BrdU-mediated free radicals form lesions such as single-strand breaks, double-strand breaks, and complex double-strand breaks (12). We assumed that BrdU could not contribute any biological response once high-LET produced enough dense ionization on their target. LET >100 keV/μm constitutes an overdose as excess ionizing events do not efficiently produce DSBs (41-43).

These results indicate that there was no detectable difference in the amount of DNA double-strand break formation and no detectable effects for repair kinetics for high-LET radiation with or without BrdU incorporation. These results were directly correlated to no differences in the frequency of chromosomal aberrations in metaphase chromosomes and cellular lethality for high LET radiation with or without BrdU substitution (Fig. 1, Table II).

BrdU and other halogenated pyrimidines appear not to be practical sensitizers to combine with carbon ion radiotherapy due to the severe sensitization to normal tissue and the small sensitization to cancer at higher LET radiation. But LET for the spread out Bragg peak for carbon ion radiotherapy contains a wide range of LET (32,34,44). In this range we would expect some sensitization for tumor control but the SER would not be as high as that for low-LET radiation such as photon and proton radiation.

Acknowledgments

We thank Dr Jamie Bush and Mr. Charles Yurkon of Colorado State University for proofreading our manuscript. This study was partially supported by the Japan Society for the Promotion of Science Grant in Aid (Young Scientists B19710056 to T.K.) and by start-up funds from Colorado State University and Dr Akiko M. Ueno Radiation Biology Research Fund. This study was part of a Research Project with Heavy Ions at the NIRS (National Institute of Radiological Sciences)-HIMAC.

References

1. Mitchell JB, Russo A, Cook JA, Straus KL and Glatstein E: Radiobiology and clinical application of halogenated pyrimidine radiosensitizers. Int J Radiat Biol 56: 827-836, 1989.
2. Franken NA, Van Bree CV, Kipp JB and Barendsen GW: Modification of potentially lethal damage in irradiated Chinese hamster V79 cells after incorporation of halogenated pyrimidines. Int J Radiat Biol 72: 101-109, 1997.
3. McLaughlin PW, Lawrence TS, Seabury H, *et al*: Bromodeoxyuridine-mediated radiosensitization in human glioma: the effect of concentration, duration, and fluoropyrimidine modulation. Int J Radiat Oncol Biol Phys 30: 601-607, 1994.
4. Kinsella TJ, Dobson PP, Mitchell JB and Fornace AJ Jr: Enhancement of X ray-induced DNA damage by pre-treatment with halogenated pyrimidine analogs. Int J Radiat Oncol Biol Phys 13: 733-739, 1987.
5. Zeng Y and Wang Y: UVB-induced formation of intrastrand cross-link products of DNA in MCF-7 cells treated with 5-bromo-2'-deoxyuridine. Biochemistry 46: 8189-8195, 2007.
6. Zeng Y and Wang Y: Sequence-dependent formation of intrastrand crosslink products from the UVB irradiation of duplex DNA containing a 5-bromo-2'-deoxyuridine or 5-bromo-2'-deoxycytidine. Nucleic Acids Res 34: 6521-6529, 2006.
7. Puck TT and Kao FT: Genetics of somatic mammalian cells. V. Treatment with 5-bromodeoxyuridine and visible light for isolation of nutritionally deficient mutants. Proc Natl Acad Sci USA 58: 1227-1234, 1967.
8. Iliakis G, Pantelias G and Kurtzman S: Mechanism of radiosensitization by halogenated pyrimidines: effect of BrdU on cell killing and interphase chromosome breakage in radiation-sensitive cells. Radiat Res 125: 56-64, 1991.
9. Webb CF, Jones GD, Ward JF, Moyer DJ, Aguilera JA and Ling LL: Mechanisms of radiosensitization in bromodeoxyuridine-substituted cells. Int J Radiat Biol 64: 695-705, 1993.
10. Zimbrick JD, Ward JF and Myers LS Jr: Studies on the chemical basis of cellular radiosensitization by 5-bromouracil substitution in DNA. I. Pulse- and steady-state radiolysis of 5-bromouracil and thymine. Int J Radiat Biol Relat Stud Phys Chem Med 16: 505-523, 1969.
11. Zimbrick JD, Ward JF and Myers LS Jr: Studies on the chemical basis of cellular radiosensitization by 5-bromouracil substitution in DNA. II. Pulse- and steady state radiolysis of bromouracil-substituted and -unsubstituted DNA. Int J Radiat Biol Relat Stud Phys Chem Med 16: 525-534, 1969.
12. Watanabe R and Nikjoo H: Modelling the effect of incorporated halogenated pyrimidine on radiation-induced DNA strand breaks. Int J Radiat Biol 78: 953-966, 2002.
13. Jones GD, Ward JF, Limoli CL, Moyer DJ and Aguilera JA: Mechanisms of radiosensitization in iododeoxyuridine-substituted cells. Int J Radiat Biol 67: 647-653, 1995.
14. Iliakis G, Wang Y, Pantelias GE and Metzger L: Mechanism of radiosensitization by halogenated pyrimidines: effect of BrdU on repair of DNA breaks, interphase chromatin breaks, and potentially lethal damage in plateau-phase CHO cells. Radiat Res 129: 202-211, 1992.
15. Iliakis G, Kurtzman S, Pantelias G and Okayasu R: Mechanism of radiosensitization by halogenated pyrimidines: effect of BrdU on radiation induction of DNA and chromosome damage and its correlation with cell killing. Radiat Res 119: 286-304, 1989.
16. Iliakis G and Kurtzman S: Mechanism of radiosensitization by halogenated pyrimidines: bromodeoxyuridine and beta-arabinofuranosyladenine affect similar subsets of radiation-induced potentially lethal lesions in plateau-phase Chinese hamster ovary cells. Radiat Res 127: 45-51, 1991.
17. Blakely EA and Kronenberg A: Heavy-ion radiobiology: new approaches to delineate mechanisms underlying enhanced biological effectiveness. Radiat Res 150: S126-S145, 1998.
18. Eguchi-Kasai K, Murakami M, Itsukaichi H, *et al*: Repair of DNA double-strand breaks and cell killing by charged particles. Adv Space Res 22: 543-549, 1998.

19. Tsujii H, Mizoe JE, Kamada T, *et al*: Overview of clinical experiences on carbon ion radiotherapy at NIRS. Radiother Oncol 73 (Suppl 2): S41-S49, 2004.
20. Jakel O: The relative biological effectiveness of proton and ion beams. Z Med Phys 18: 276-285, 2008.
21. Prise KM, Pinto M, Newman HC and Michael BD: A review of studies of ionizing radiation-induced double-strand break clustering. Radiat Res 156: 572-576, 2001.
22. Fakir H, Sachs RK, Stenerlow B and Hofmann W: Clusters of DNA double-strand breaks induced by different doses of nitrogen ions for various LETs: experimental measurements and theoretical analyses. Radiat Res 166: 917-927, 2006.
23. Hada M and Georgakilas AG: Formation of clustered DNA damage after high-LET irradiation: a review. J Radiat Res 49: 203-210, 2008.
24. Pinto M, Prise KM and Michael BD: Evidence for complexity at the nanometer scale of radiation-induced DNA DSBs as a determinant of rejoining kinetics. Radiat Res 164: 73-85, 2005.
25. Linstadt D, Blakely E, Phillips TL and Castro JR: Radiosensitization produced by iododeoxyuridine with high linear energy transfer heavy ion beams. Int J Radiat Oncol Biol Phys 15: 703-710, 1988.
26. Oliveira NG, Castro M, Rodrigues AS, *et al*: Wortmannin enhances the induction of micronuclei by low and high LET radiation. Mutagenesis 18: 37-44, 2003.
27. Skarsgard LD: Radiobiology with heavy charged particles: a historical review. Phys Med 14 (Suppl 1): 1-19, 1998.
28. Hamada N, Imaoka T, Masunaga S, *et al*: Recent advances in the biology of heavy-ion cancer therapy. J Radiat Res 51: 365-383, 2010.
29. Nagasawa H and Little JB: Effect of tumor promoters, protease inhibitors, and repair processes on X-ray-induced sister chromatid exchanges in mouse cells. Proc Natl Acad Sci USA 76: 1943-1947, 1979.
30. Terasima T and Tolmach LJ: Changes in X-ray sensitivity of HeLa cells during the division cycle. Nature 190: 1210-1211, 1961.
31. Kanai T, Endo M, Minohara S, *et al*: Biophysical characteristics of HIMAC clinical irradiation system for heavy-ion radiation therapy. Int J Radiat Oncol Biol Phys 44: 201-210, 1999.
32. Kanai T, Matsufuji N, Miyamoto T, *et al*: Examination of GyE system for HIMAC carbon therapy. Int J Radiat Oncol Biol Phys 64: 650-656, 2006.
33. Matsufuji N, Fukumura A, Komori M, Kanai T and Kohno T: Influence of fragment reaction of relativistic heavy charged particles on heavy-ion radiotherapy. Phys Med Biol 48: 1605-1623, 2003.
34. Matsufuji N, Kanai T, Kanematsu N, *et al*: Specification of carbon ion dose at the National Institute of Radiological Sciences (NIRS). J Radiat Res 48 (Suppl A): A81-A86, 2007.
35. Rogakou EP, Boon C, Redon C and Bonner WM: Megabase chromatin domains involved in DNA double-strand breaks in vivo. J Cell Biol 146: 905-915, 1999.
36. Rogakou EP, Boon C and Bonner WM: Formation of a novel histone derivative, H2AX phosphorylated on serine-139, is an immediate cellular response to non-lethal and lethal amounts of ionizing radiation, and is also found during apoptosis and in germ cells. Mol Biol Cell 8: 1858-1858, 1997.
37. Banath JP, MacPhail SH and Olive PL: Radiation sensitivity, H2AX phosphorylation, and kinetics of repair of DNA strand breaks in irradiated cervical cancer cell lines. Cancer Res 64: 7144-7149, 2004.
38. Kuhne M, Riballo E, Rief N, Rothkamm K, Jeggo PA and Lobrich M: A double-strand break repair defect in ATM-deficient cells contributes to radiosensitivity. Cancer Res 64: 500-508, 2004.
39. Kato TA, Nagasawa H, Weil MM, Little JB and Bedford JS: Levels of gamma-H2AX foci after low-dose-rate irradiation reveal a DNA DSB rejoining defect in cells from human ATM heterozygotes in two at families and in another apparently normal individual. Radiat Res 166: 443-453, 2006.
40. Wang Y, Pantelias GE and Iliakis G: Mechanism of radiosensitization by halogenated pyrimidines: the contribution of excess DNA and chromosome damage in BrdU radiosensitization may be minimal in plateau-phase cells. Int J Radiat Biol 66: 133-142, 1994.
41. Prise KM, Folkard M, Newman HC and Michael BD: Effect of radiation quality on lesion complexity in cellular DNA. Int J Radiat Biol 66: 537-542, 1994.
42. Chapman JD, Doern SD, Reuvers AP, *et al*: Radioprotection by DMSO of mammalian cells exposed to X-rays and to heavy charged-particle beams. Radiat Environ Biophys 16: 29-41, 1979.
43. Yang TC, Craise LM, Mei MT and Tobias CA: Neoplastic cell transformation by heavy charged particles. Radiat Res Suppl 8: S177-S187, 1985.
44. Fukumura A, Tsujii H, Kamada T, *et al*: Carbon-ion radiotherapy: clinical aspects and related dosimetry. Radiat Prot Dosimetry 137: 149-155, 2009.

IJC
International Journal of Cancer

Serum interleukin-6 associated with hepatocellular carcinoma risk: A nested case–control study

Waka Ohishi[1], John B. Cologne[2], Saeko Fujiwara[1,3], Gen Suzuki[4], Tomonori Hayashi[5], Yasuharu Niwa[5], Masazumi Akahoshi[6], Keiko Ueda[1], Masataka Tsuge[7] and Kazuaki Chayama[7]

[1] Department of Clinical Studies, Radiation Effects Research Foundation, Hiroshima, Japan
[2] Department of Statistics, Radiation Effects Research Foundation, Hiroshima, Japan
[3] Health Management and Promotion Center, Hiroshima Atomic Bomb Casualty Council, Hiroshima, Japan
[4] International University of Health and Welfare Clinic, Ohtawara, Japan
[5] Department of Radiation Biology and Molecular Epidemiology, Radiation Effects Research Foundation, Hiroshima, Japan
[6] Department of Clinical Studies, Radiation Effects Research Foundation, Nagasaki, Japan
[7] Department of Gastroenterology and Metabolism, Applied Life Sciences, Institute of Biomedical and Health Sciences, Hiroshima University, Hiroshima, Japan

Inflammatory markers have been associated with increased risk of several cancers, including colon, lung, breast and liver, but the evidence is inconsistent. We conducted a nested case–control study in the longitudinal cohort of atomic-bomb survivors. The study included 224 hepatocellular carcinoma (HCC) cases and 644 controls individually matched to cases on gender, age, city and time and method of serum storage, and countermatched on radiation dose. We measured C-reactive protein (CRP) and interleukin (IL)-6 using stored sera obtained within 6 years before HCC diagnosis from 188 HCC cases and 605 controls with adequate volumes of donated blood. Analyses with adjustment for hepatitis virus infection, alcohol consumption, smoking habit, body mass index (BMI) and radiation dose showed that relative risk (RR) of HCC [95% confidence interval (CI)] in the highest tertile of CRP levels was 1.94 (0.72–5.51) compared to the lowest tertile ($p = 0.20$). RR of HCC (95% CI) in the highest tertile of IL-6 levels was 5.12 (1.54–20.1) compared to the lowest tertile ($p = 0.007$). Among subjects with BMI > 25.0 kg/m^2, a stronger association was found between a 1-standard deviation (SD) increase in log IL-6 and HCC risk compared to subjects in the middle quintile of BMI (21.3–22.9 kg/m^2), resulting in adjusted RR (95% CI) of 3.09 (1.78–5.81; $p = 0.015$). The results indicate that higher serum levels of IL-6 are associated with increased HCC risk, independently of hepatitis virus infection, lifestyle-related factors and radiation exposure. The association is especially pronounced among subjects with obesity.

Epidemiology

Key words: C-reactive protein, interleukin-6, obesity, hepatocellular carcinoma, nested case–control study

Abbreviations: BMI: body mass index; CI: confidence interval; CRP: C-reactive protein; HBV: hepatitis B virus; HCC: hepatocellular carcinoma; HCV: hepatitis C virus; IL-6: interleukin-6; RERF: Radiation Effects Research Foundation; RR: relative risk; SD: standard deviation

Conflict of interest: Nothing to report

Grant sponsor: Japanese Ministry of Education, Culture, Sports, Science and Technology; **Grant number:** 20590672; **Grant sponsor:** U.S. Department of Energy (DOE); **Grant number:** DE-HS0000031; **Grant sponsors:** RERF Research Protocols #2-75 and #1-09, Japanese Ministry of Health, Labour and Welfare (MHLW)

DOI: 10.1002/ijc.28337

History: Received 30 Mar 2013; Accepted 31 May 2013; Online 20 Jun 2013

Correspondence to: Waka Ohishi, MD, PhD, Department of Clinical Studies, Radiation Effects Research Foundation, 5-2 Hijiyama Park, Minami-ku, Hiroshima 732-0815, Japan, Tel.: +81-82-261-9122, Fax: +81-82-261-3259, E-mail: nwaka@rerf.or.jp

Hepatocellular carcinoma (HCC) is one of the most common cancers worldwide. Chronic infections with hepatitis B virus (HBV) or hepatitis C virus (HCV) are recognized as crucially important risk factors for HCC, whereas an increase of HCC without HBV and HCV infection (non-B, non-C HCC) has been noted recently in Japan.[1,2] Although periodic follow-up with imaging, tumor markers such as alpha-fetoprotein (AFP) and fibrosis markers are recommended, these strategies have not been sufficient for early detection of HCC in chronic liver disease, especially in non-B, non-C liver disease. Therefore, it is necessary to identify biomarkers that may be useful to narrow down a high-risk subgroup for HCC.

A large number of epidemiologic studies have shown that obesity and diabetes mellitus are associated with increased risks of such malignant tumors as colon, prostate and breast, as well as HCC.[3–11] Our earlier study also demonstrated that obesity [body mass index (BMI) > 25.0 kg/m^2] 10 years before HCC diagnosis was significantly associated with increased risk of HCC, independently of HBV and HCV infection, alcohol consumption, smoking habit and radiation exposure.[12] It has been suggested that cell proliferation activity of insulin due to hyperinsulinemia or chronic inflammation may promote

What's new?

According to previous research, alcohol consumption, obesity, and radiation exposure as well as hepatitis virus infection are all independent risk factors for hepatocellular carcinoma (HCC). Inflammatory markers have also been associated with increased risk of liver cancer, but the evidence is inconsistent. In this nested case-control study in the longitudinal cohort of atomic-bomb survivors, which took into account hepatitis virus infection, lifestyle-related factors, and radiation exposure, elevated IL-6 levels were found to be associated with increased risk of HCC. The findings also indicated that association of IL-6 levels with increased risk of HCC is especially pronounced among subjects with obesity.

carcinogenesis by DNA damage, enhancement of cellular proliferation and inhibition of apoptosis.[4,13] In recent years, some studies have suggested that blood levels of inflammatory markers or cytokines also related to insulin resistance—such as C-reactive protein (CRP), interleukin (IL)-6 and tumor necrosis factor (TNF)—may reveal a biological mechanism by which risks of colon, lung and breast cancers increase,[14–17] but other studies have not supported such associations.[18,19]

Several studies have demonstrated that elevated serum levels of IL-6 are associated with increased risk of HCC in female chronic hepatitis C patients,[20] and that the combination of serum levels of IL-6 and alpha-fetoprotein improves sensitivity in diagnosing HCC or predicting future HCC development in chronic hepatitis B patients.[21] A few experimental studies using a mouse model have demonstrated that estrogen-mediated inhibition of IL-6 production by Kupffer cells reduces liver cancer risk in females,[22] and that obesity-promoted HCC development was bound up with elevated production of the tumor-promoting cytokines, such as IL-6 and TNF, which cause hepatic inflammation and activation of the oncogenic transcription factor STAT3.[23] In several other cancers,[24,25] it has been suggested that IL-6 and STAT3 may also contribute toward a general enhancement of cancer risk by high BMI.

With the aim of investigating whether serum levels of CRP and IL-6 are associated with risk of HCC and, if so, whether that risk is independent of HBV and HCV infection, alcohol consumption, smoking habit, BMI and radiation exposure, we conducted a nested case–control study using sera collected from a prospective cohort study of atomic-bomb survivors. We subsequently evaluated whether the association between serum IL-6 levels and HCC risk is modified by alcohol consumption, smoking habit, BMI or radiation dose to the liver using analyses based on subgroups of those factors.

Material and Methods

Cohorts

The Atomic Bomb Casualty Commission (ABCC) and its successor, the Radiation Effects Research Foundation (RERF), established the prospective Adult Health Study cohort in 1958, in which more than 20,000 gender-, age- and city-matched proximal and distal atomic-bomb survivors and persons not present in the cities at the time of bombings have been examined biennially in outpatient clinics in Hiroshima and Nagasaki.

Cases and controls

Incident cancer cases were identified through the Hiroshima Tumor and Tissue Registry and Nagasaki Cancer Registry, confirmed and supplemented by additional cases detected *via* pathological review of related diseases.[26] As described in our previous studies,[3,27] 359 primary HCC cases were diagnosed among 18,660 Adult Health Study participants between 1970 and 2002, who visited our outpatient clinics before their diagnosis. Of these, 229 cases had serum samples obtained within 6 years before HCC diagnosis (average: stored sera obtained 1.2 years before diagnosis). After excluding five cases with inadequate stored serum, 224 cases remained for our previous studies. There were no important differences in characteristics such as alcohol consumption, smoking habit, BMI or radiation dose to the liver (among exposed persons) between HCC cases excluded because of nonavailability of stored serum and those included in our study.

As described in our previous studies,[3,27] 644 controls were selected from the at-risk cohort members matched to the case on gender, age, city and time and method of serum storage, and countermatched on radiation dose in nested case–control fashion.[28] Counter matching (to increase statistical efficiency for studying joint effects of radiation and other factors) was performed using four strata based on whole-body (skin) dose: zero dose (<0.0005 Gy), <0.05 Gy, <0.75 Gy and ≥ 0.75 Gy (nonzero categories correspond roughly to tertiles of skin dose among all eligible exposed cases). At the time of each case diagnosis, one control serum was selected at random from each of the three dose strata not occupied by the case in the cohort risk set.

Laboratory tests

Virological assays of HBV and HCV were performed on 211 cases and 640 controls with sufficient stored sera for these assays as previously described.[29,30] HBV infection (HBV+) status was defined as positive for HBsAg or having a high titer of anti-HBc Ab (positive for anti-HBc Ab of samples diluted 200-fold). HCV infection (HCV+) status was defined as positive for HCV RNA. Non-B, non-C status was defined as negative for HBsAg and not having a high titer of anti-HBc Ab (HBV-) as well as negative for HCV RNA (HCV-).

Serum levels of CRP were measured using an autoanalyzer (Hitachi 7180, Hitachi, Tokyo, Japan) and a high-sensitivity assay kit (Nissui Pharmaceutical, Tokyo, Japan) containing anti-CRP monoclonal antibodies. The detection limit of CRP was 0.08 mg/L. The intra-assay variability was determined by assaying two pooled serum samples (mean CRP level: 0.62 and 1.68 mg/L, respectively) 20 times in a single day, and the respective coefficients of variation (CVs) were 1.12 and 0.95%. The interassay variability was determined by assaying two quality control samples (mean CRP level: 2.14 and 4.71 mg/L, respectively) once a day 12 for days; the respective CVs were 4.1 and 1.2%. Serum levels of IL-6 were measured using the multiplex bead array assay on the Luminex Complete System 200 (Luminex Corp., Austin, TX),[31] with MILLIPLEX™ MAP kits (Millipore, Billerica, MA) according to the manufacturer's instructions. Human serum adipokine panel B (HADK2-61K-B) was used for IL-6. The intra-assay variability was determined by assaying two pooled serum samples with and without including a quality control sample (mean IL-6 level: 4.29 and 144.82 pg/mL, respectively) 15 times in a single day, and the respective CVs were 8.6 and 7.5%. The interassay variability was determined by assaying two quality control samples (mean IL-6 level: 31.02 and 171.62 pg/mL, respectively) once a day for 7 days; the respective CVs were 7.9 and 13.7%.

Radiation dose

Radiation dose to the liver was estimated for each subject according to Dosimetry System DS02.[32] A weighted sum of the gamma dose in gray plus ten times the neutron dose in gray was used.

Alcohol consumption, smoking habit and BMI

Self-administrated questionnaires on lifestyle-related factors were given to Adult Health Study participants in 1965 during attendance at the outpatient clinic and in 1978 by mail survey. Information on alcohol consumption was obtained from the 1965 questionnaire when available, with missing data complemented using the 1978 mail survey. Mean ethanol amounts were calculated as grams per day, as previously described.[33] Information on smoking habit was obtained from the 1965 questionnaire. Subjects were categorized as never, current or former smoker. BMI (kg/m^2) was calculated from height and weight measured in the outpatient clinic of the Adult Health Study. Subjects were classified based on BMI quintiles with cut points of 19.5, 21.2, 22.9 and 25.0. Following the recommendations for Asian people by the WHO, the International Association for the Study of Obesity and the International Obesity Task Force,[34] 21.3–22.9 kg/m^2 was considered as normal, 23.0–25.0 kg/m^2 as overweight and >25.0 kg/m^2 as obese.

Ethical consideration

This study (RERF Research Protocol 1-09) was reviewed and approved by the Research Protocol Review Committee and the Human Investigation Committee of RERF.

Statistical analyses

The nested case–control design is analyzed using a partial likelihood method analogous to that used for cohort follow-up studies,[35] which is in practice the same as the conditional binary data likelihood for matched case–control studies[36] except that the subjects (cases and controls) in the study are not completely independent owing to the possibility of repeated selection. Radiation risk was estimated using an excess relative risk (ERR) model (ERR = RR − 1) to conform to other analyses of the atomic-bomb survivor cohort.[3,27,37] Bias in control doses due to selecting controls using countermatching was corrected using weights as described elsewhere.[28] Risks for all other factors were assessed using a log-linear model. In analyses based on continuous values, CRP and IL-6 were transformed using the natural logarithm. Analyses using CRP or IL-6 groups used tertiles computed among controls. A two-degree-of-freedom heterogeneity test was performed by comparing the deviance of the model with tertiles to that without, using the lowest tertile as the comparison group. We fit log-linear regression models for the effect of a 1-standard deviation (SD) increase in IL-6 and tested for interaction with each of the other risk factors individually using the same heterogeneity test, with degrees of freedom depending on the number of categories of the other risk factor; we report the p value for the pairwise test comparing the interaction parameter in the highest to lowest level of each other risk factor. We also assessed various models for log relative risk of HCC with continuous level of IL-6—linear, linear-quadratic and linear spline—using the Akaike information criterion (AIC).[38] Analyses were conducted using Epicure (HIROSOFT International Corp., Seattle, WA).

Results

Characteristics of cases and controls

Table 1 shows characteristics of HCC cases and matched controls. Because of matching, cases and controls were comparable with respect to gender, age, city and time and method of serum storage. Prevalence of HBV and/or HCV infection status in HCC cases is higher than in controls. Compared to the controls, higher proportions of HCC cases had a history of alcohol consumption exceeding 40 g of ethanol per day, were obese (BMI > 25.0 kg/m^2) and were current smokers. Median serum levels of CRP were 0.72 mg/L among HCC cases and 0.59 mg/L among controls. Median serum levels of IL-6 were 4.88 pg/mL among HCC cases and 2.90 pg/mL among controls. HCC cases also received on average higher radiation doses to the liver compared to controls.

Correlations among CRP, IL-6, alcohol, BMI and radiation dose

Table 2 shows Spearman rank-correlation coefficients (r) between serum levels of CRP and IL-6, alcohol consumption,

Table 1. Characteristics of HCC cases and controls

Study variables	HCC cases		Controls	
	Number with complete data	*n* (%)	Number with complete data	*n* (%)
Matched variables				
Age at HCC diagnosis (years)[1]	224	67.6 (10.1)	–	–
Age at serum storage (years)[1]	224	66.4 (10.2)	644	63.7 (9.8)
Gender	224		644	
Male		136 (60.7)		387 (60.1)
Female		88 (39.3)		257 (39.9)
City	224		644	
Hiroshima		155 (69.2)		444 (68.9)
Nagasaki		69 (30.8)		200 (31.1)
Unmatched variables				
Viral etiology	211		640	
HBV−/HCV−		45 (21.3)		579 (90.5)
HBV+ and/or HCV+		166 (78.7)		61 (9.5)
Alcohol consumption (g ethanol/day)	199		577	
None		97 (48.7)		315 (54.6)
0< <40		57 (28.6)		194 (33.6)
≥40		45 (22.6)		68 (11.8)
Smoking habit	199		578	
Never		80 (40.2)		283 (49.0)
Current smoker		107 (53.8)		262 (45.3)
Former smoker		12 (6.0)		33 (5.7)
BMI (kg/m^2) 10 years before diagnosis	210		633	
≤19.5		38 (18.1)		122 (19.3)
19.6–21.2		33 (15.7)		136 (21.5)
21.3–22.9		36 (17.2)		142 (22.4)
23.0–25.0		49 (23.3)		124 (19.6)
>25.0		54 (25.7)		109 (17.2)
Inflammatory markers				
CRP (mg/L), median (IQR)	188	0.72 (0.18, 1.89)	605	0.59 (0.25, 1.52)
IL-6 (pg/mL), median (IQR)	182	4.88 (2.88, 8.77)	589	2.90 (1.53, 5.42)
Radiation dose to the liver (Gy)[1,2]	204	0.46 (0.69)	606	0.34 (0.56)

[1]Mean (SD).
[2]Control values were adjusted for countermatched selection.

BMI 10 years before HCC diagnosis and radiation dose to the liver. Serum levels of CRP were positively correlated with serum levels of IL-6 among both cases (r = 0.46) and controls (r = 0.29). Serum levels of CRP were modestly correlated with BMI among both cases (r = 0.15) and controls (r = 0.28), whereas correlations between serum levels of IL-6 and BMI were not significant among either cases (r = 0.11) or controls (r = 0.06). Neither alcohol consumption nor radiation dose showed any evidence of correlation with either marker.

Risk of HCC according to serum levels of CRP and IL-6

Table 3 shows the association between CRP and HCC risk based on tertiles of serum CRP levels. Analyses with adjustment for HBV and HCV infection, alcohol consumption, smoking habit, BMI 10 years before HCC diagnosis and radiation dose showed that relative risks (RRs) of HCC [95% confidence interval (CI)] in the middle tertile (0.37–0.96 mg/L) and highest tertile (>0.96 mg/L) of CRP levels were 2.11 (0.73–6.54; p = 0.17) and 1.94 (0.72–5.51; p = 0.20), respectively, compared to

Table 2. Spearman rank-correlation coefficients between CRP, IL-6, alcohol, BMI and radiation dose among HCC cases and controls

Variables	CRP		IL-6	
	Correlation	*p* Value	Correlation	*p* Value
HCC cases				
CRP	–	–	–	–
IL-6	0.46	<0.001	–	–
Alcohol consumption (g ethanol/day)	0.01	0.9	−0.02	0.83
BMI 10 years before diagnosis	0.15	0.049	0.11	0.14
Radiation dose to the liver	−0.09	0.26	−0.08	0.30
Controls				
CRP	–	–	–	–
IL-6	0.29	<0.001	–	–
Alcohol consumption (g ethanol/day)	−0.003	0.94	0.05	0.28
BMI 10 years before diagnosis	0.28	<0.001	0.06	0.13
Radiation dose to the liver	−0.02	0.64	−0.06	0.13

Table 3. Relative risks of HCC by tertile of serum levels of CRP

	Tertile of CRP			*p* Value for heterogeneity
	Low < 0.37 mg/L	Middle 0.37–0.96 mg/L	High > 0.96 mg/L	
No. of cases/controls[1]	**49/120**	**29/98**	**59/109**	
Crude RR (95% CI)	1.00	0.64 (0.36–1.15)	1.16 (0.71–1.88)	0.10
p Value	–	0.14	>0.50	
Adjusted RR (95% CI)[2]	1.00	1.54 (0.62–3.92)	1.90 (0.87–4.36)	0.28
p Value	–	0.36	0.11	
Adjusted RR (95% CI)[3]	1.00	2.11 (0.73–6.54)	1.94 (0.72–5.51)	0.32
p Value	–	0.17	0.20	

[1]Number of subjects for whom information available for all factors included in a log-linear model: 137 HCC cases and 327 controls.
[2]Adjusted for HBV/HCV infection, excluding three HBV+/HCV+ individuals.
[3]Adjusted for HBV/HCV infection, alcohol consumption, smoking habit, BMI 10 years before diagnosis and radiation dose to the liver.

Table 4. Relative risks of HCC by tertile of serum levels of IL-6

	Tertile of IL-6			*p* Value for heterogeneity
	Low < 2.01 pg/mL	Middle 2.01–4.46 pg/mL	High > 4.46 pg/mL	
No. of cases/controls[1]	**13/103**	**48/107**	**71/103**	
Crude RR (95% CI)	1.00	3.78 (1.87–8.26)	6.44 (3.24–14.0)	<0.001
p Value	–	<0.001	<0.001	
Adjusted RR (95% CI)[2]	1.00	2.87 (1.02–8.91)	4.09 (1.46–12.9)	0.025
p Value	–	0.045	0.007	
Adjusted RR (95% CI)[3]	1.00	3.85 (1.16–14.7)	5.12 (1.54–20.1)	0.023
p Value	–	0.027	0.007	

[1]Number of subjects for whom information available for all factors included in a log-linear model: 132 HCC cases and 313 controls.
[2]Adjusted for HBV/HCV infection, excluding three HBV+/HCV+ individuals.
[3]Adjusted for HBV/HCV infection, alcohol consumption, smoking habit, BMI 10 years before diagnosis and radiation dose to the liver.

those in the lowest tertile (<0.37 mg/L; heterogeneity $p = 0.32$).

Table 4 shows the association between IL-6 and HCC risk based on tertiles of IL-6. Analyses with adjustment for HBV and HCV infection, alcohol consumption, smoking habit, BMI 10 years before HCC diagnosis and radiation dose showed that RRs of HCC (95% CI) in the middle tertile (2.01–4.46 pg/mL) and highest tertile (>4.46 mg/L) of IL-6

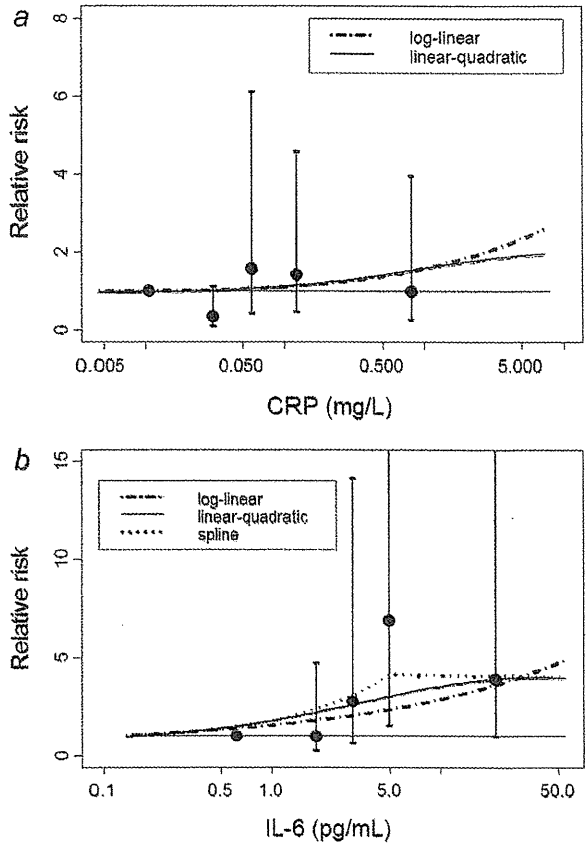

Figure 1. (*a*) Continuous risk of HCC by CRP. RR (95% CI) of HCC with adjustment for alcohol, smoking habit, BMI and radiation dose is plotted according to serum levels of CRP. A test for overall significance of the log-linear curve was not significant (p = 0.23, dashed line). Fit of a linear-quadratic model (solid line) was not as good as the log-linear model according to the AIC model-comparison criterion. (*b*) Continuous risk of HCC by IL-6. RR (95% CI) of HCC with adjustment for alcohol, smoking habit, BMI and radiation dose is plotted according to serum levels of IL-6. A test for overall significance of the log-linear curve was significant (p = 0.015, dashed line). Fits of linear-quadratic (solid line) and linear spline (dotted line) were not as good as the log-linear model according to the AIC model-comparison criterion.

levels were 3.85 (1.16–14.7; p = 0.027) and 5.12 (1.54–20.1; 0.007), respectively, compared to those in the lowest tertile (<2.01 pg/mL; heterogeneity p = 0.023).

Additional analyses were conducted to examine the association between CRP or IL-6 and non-B, non-C HCC risk, although there were relatively few cases with non-B, non-C status (31 cases). Analyses with adjustment for alcohol consumption, smoking habit, BMI 10 years before HCC diagnosis and radiation dose showed that RRs of non-B, non-C HCC (95% CI) in the middle and highest tertiles of CRP were 7.77 (1.13–78.5) and 7.40 (1.26–64.6), respectively, compared to those in the lowest tertile (heterogeneity p = 0.065). RRs of non-B, non-C HCC (95% CI) in the middle and highest tertiles of IL-6 were 56.3 (4.27–2,000) and 98.0 (6.74–4,500), respectively, compared to those in the lowest tertile (heterogeneity $p < 0.001$) after the same adjustment. The wide confidence bounds are presumably due to the small numbers of non-B, non-C HCC cases.

We also examined the possibility of a nonlinear relation between serum levels of CRP or IL-6 and HCC risk. There was no evidence of any systematic relationship between CRP and HCC risk (Fig. 1*a*). The log RR of HCC increased linearly with logarithm of serum IL-6 level after adjustment for alcohol consumption, smoking habit, BMI and radiation dose (p = 0.015, AIC = 132.63; Fig.1*b*). Although HCC risk appears to level off or decline at high values of IL-6 (Fig.1*b*), neither a negative quadratic term (p = 0.17, AIC = 132.73) nor a linear spline (p = 0.10, AIC = 133.95, with best fit obtained using a join point at log IL-6 = 1.6 or IL-6 = 4.95) revealed any statistically significant departure from the log-linear model. Although the appearance of a downturn at high values of IL-6 may be spurious, lack of statistical significance could also be due to the large uncertainty in estimated risk for IL-6 (high upper bound on confidence intervals for IL-6 groups).

Interaction between IL-6 level and gender, lifestyle-related factors or radiation for risks of HCC

Table 5 shows the association between IL-6 and HCC risk by selected subgroups. Stronger association was found between a 1-SD increase in log IL-6 and HCC risk among subjects with BMI of >25.0 kg/m^2 (obese) 10 years before diagnosis than among subjects with BMI of 21.3–22.9 kg/m^2 (normal), resulting in adjusted RR (95% CI) of 3.09 (1.78–5.81; p for interaction = 0.015). However, there was no significant difference in association between IL-6 and HCC risk among females compared to males, among subjects with alcohol consumption of 40 g of ethanol per day compared to never drinkers, among current smokers compared to never smokers or among subjects exposed to ≥1.0 Gy radiation compared to subjects exposed to <0.001 Gy radiation.

Additional analyses were conducted to examine the association between IL-6 and non-B, non-C HCC risk by selected subgroups. Similarly, a stronger association was found between a 1-SD increase in log IL-6 and non-B, non-C HCC risk among subjects with BMI of >25.0 kg/m^2 than among subjects with BMI of 21.3–22.9 kg/m^2, resulting in adjusted RR (95% CI) of 5.01 (1.51–34.0; p for interaction = 0.025). The results suggest that elevated serum levels of IL-6 among obese subjects are more strongly associated with increased risks of non-B, non-C HCC as well as overall HCC compared to subjects with normal weight.

Discussion

Our study demonstrated that elevated serum levels of IL-6 are associated with increased risk of HCC, independently of hepatitis virus infection, lifestyle-related factors—such as alcohol consumption, smoking habit and BMI—and radiation